



Synthesis, characterization, and *in vitro* release of oxytetracycline loaded in pH-responsive CaCO₃ nanoparticles

Sherifat Banke Idris^{1,6}, Arifah Abdul Kadir^{*}, Faez Firdaus Abdullah Jesse², Siti Zubaidah Ramanoon³, Muhammad Abdul Basit^{1,7}, Zainul Amiruddin Zakaria⁴, Md Zuki Abu Bakar Zakaria^{1,5}

¹Department of Veterinary Preclinical Sciences, Faculty of Veterinary Medicine, Universiti Putra Malaysia, Serdang, Malaysia.

²Department of Veterinary Clinical Studies, Faculty of Veterinary Medicine, Universiti Putra Malaysia, 43400 UPM Serdang, Malaysia.

³Department of Farm and Exotic Animal Medicine and Surgery, Faculty of Veterinary Medicine, Universiti Putra Malaysia, 43400 UPM Serdang, Malaysia.

⁴Department of Biomedical Sciences, Faculty of Medicine and Health Sciences, Universiti Putra Malaysia, 43400 UPM Serdang, Malaysia.

⁵Institute of Biosciences, Universiti Putra Malaysia, 43400 UPM Serdang, Malaysia.

⁶Department of Veterinary Pharmacology and Toxicology, Faculty of veterinary Medicine, Usmanu Danfodiyo University, Sokoto, Nigeria.

⁷Department of Biosciences, Faculty of Veterinary Sciences, Bahauddin Zakariya University, Multan, Pakistan.

ARTICLE INFO

Received on: 18/03/2019

Accepted on: 06/06/2019

Available online: 04/11/2019

Key words:

CaCO₃ nanoparticle, oxytetracycline, morphological characterization, drug loading, *in vitro* release.

ABSTRACT

Alternative drug delivery for the treatment of resistant bacterial infections is necessary to bypass existing antibiotic resistance mechanism and ensure direct delivery of the drug to the targeted site using locally sourced materials to minimize cost in the long term. In this study, cockle shell-derived calcium carbonate aragonite nanoparticles (CS-CaCO₃NP) was synthesized, loaded with oxytetracycline (OTC), and characterized using Zeta analysis, Transmission electron microscopy (TEM), FESEM, X-ray Diffraction (XRD), Fourier Transform Infrared (FTIR) and Brunauer–Emmett–Teller analysis. The loaded OTC-CS-CaCO₃NP was further characterized after which the *in vitro* release of OTC was studied. A homogenously spherical CS-CaCO₃NP was observed on TEM with a mean diameter of 29.90 nm and -19.9 zeta potential which increased to 62.40 nm and -23.5, respectively, after OTC loading. XRD and FTIR analysis of OTC-CS-CaCO₃NP revealed that OTC maintained its functionality and crystallinity. The formulation of OTC:CS-CaCO₃NP in ratio 1:4 with drug encapsulating efficiency (71%) was used for *in vitro* release studies. OTC was sustainably released from OTC-CS-CaCO₃NP over a period of 96 hours. Our results suggest that OTC-CS-CaCO₃NP is a promising nanoparticle antibiotic delivery system with efficient physicochemical and pharmacological properties whose antibiotic properties should be further investigated.

INTRODUCTION

Cockle shells derived from bivalve mollusks or *Anadara granosa* are a waste product of Malaysian aquaculture industry (Othman *et al.*, 2013). The quest to reduce waste and looking inwards for alternative uses of this abundant natural reserve of calcium carbonate, the main chemical constituent of cockle shells, has resulted in its wide application in the field of engineering, pharmacology, and medicine (Razalia *et al.*, 2016).

Biocompatibility of calcium carbonate has been described and this makes it a perfect candidate for nano drug delivery (Kamba *et al.*, 2013). Direct bactericidal activity of nanoparticles which results in improved therapeutic index and efficacy has prompted the loading of antibiotics into calcium carbonate nanoparticles with the aim of better treatment while reducing costs (Isa *et al.*, 2016; Saidykhani *et al.*, 2016).

Oxytetracycline (OTC) is a very common antibiotic widely used in veterinary medicine for the treatment of bacterial infections caused by both Gram-positive and Gram-negative organisms; however, the emergence of resistant strains has questioned its therapeutic effects (Larbi-Bouamrane *et al.*, 2016). Employing the use of nanoparticles to deliver antibiotics in the treatment of bacterial infections has yielded good results due to the

^{*}Corresponding Author

Arifah Abdul Kadir, Department of Veterinary Preclinical Sciences Faculty of Veterinary Medicine, Universiti Putra Malaysia, Serdang, Malaysia.
E-mail: arifah@upm.edu.my

unique properties of nanoparticles such as ultra-small size, large surface to mass area, and bacterial membrane adhering properties (Adhikari *et al.*, 2013). More so, the successful synthesis of nanoparticles loaded drug with right physicochemical properties for effective *in vitro* and *in vivo* interactions rely on the methods of synthesis. Different methods of synthesizing nanoparticles have been described and all revolve mainly around a top- or bottom-down approach. For the top-down approach, the fabrication of nanoparticles usually starts from the large-sized raw material and is broken down to the level of desired size of nanoparticles as the end product or from a bottom-up approach where individual elements to make diverse fine nanoparticles are synthesized from scratch, while the bottom down approach entails the synthesis of these nanoparticles from individual elements (Dhand *et al.*, 2015; Priyadarshana *et al.*, 2015). Three processes are basically used for the synthesis, namely, physical, biological, and mechanical process. In the physical method, heat, gas, and vapor are applied to the precursors of the different nanoparticles through processes like gas condensation, vacuum deposition and vaporization, laser pyrolysis, melt mixing, and high energy ball rolling mill (Rawat *et al.*, 2016). The biological process involves the synthesis of nanoparticles from some microorganisms or plants while the chemical process involves nanoparticles fabrication via polyol synthesis, microemulsion technique, sol gel, and chemical vapor (Dhand *et al.*, 2015).

Using the right method of synthesis, we, therefore, hypothesize that oxytetracycline will retain its physicochemical and pharmacological properties when loaded into cockle shell-derived calcium carbonate aragonite nanoparticles (CS-CaCO₃NP). In this study, we synthesized (CS-CaCO₃NP) by a top-down approach, loaded it with oxytetracycline, and characterized it for use against livestock resistant bacteria species.

MATERIALS AND METHODS

Synthesis of CaCO₃ nanoparticles from cockle shell powder

Cockle shell was washed and milled mechanically to get micron-sized cockle shell powder as described by Danmaigoro *et al.* (2017). The prepared micron size cockle shell powder was further processed; thus, 2 g of 75 µm micron-sized powder of CS-CaCO₃ powder was weighed with an electronic balance (Biobase, BA 2204 B) and put in a flat bottom flask with a magnetic stirring bar within it. 50 ml of deionized water was added to the powder. The resultant solution was stirred on a systematic multi hot plate stirring machine (Systematic Multi-Hotplate Stirrers 6 Positions, WiseStir® Korean) set at 1,000 rpm (27°C for 2 hours). After 5 minutes of agitation, 0.5 ml of dodecyl dimethyl betaine (BS-12) Sigma-Aldrich (Steinheim, Germany) was added gradually into the solution and covered with aluminum foil. After 2 hours of stirring, the solution was filtered with filter paper of diameter 18.0 cm and the surfactant rinsed off through the filter paper with double deionized water, leaving the sediments which are the nanoparticles on the filter paper. This was then allowed to dry for 3 days in the oven at 50°C. The dried newly synthesized nanoparticle was placed in a cylindrical jar of 8 cm in diameter (with a 7 cm flat iron fixed perpendicular to it) containing 15 ceramic balls and placed on a roller mill at 200 rpm for three consecutive days overnight (54 hours). The resulting fine CS-CaCO₃ nanoparticle was then

packed in glass bottles and stored in the oven at 50°C till further analysis.

Loading of oxytetracycline into synthesized CS-CaCO₃ nanoparticles

The loading of oxytetracycline was done by mixing the free oxytetracycline and the right concentration of synthesized CS-CaCO₃NP with the aid of lab multistirrer (Systematic Multi-Hotplate Stirrers 6 Positions, WiseStir® Korean) overnight at room temperature set at 200 ± 1 rpm. After overnight mechanical agitation, the suspensions of the OTC-CS-CaCO₃NP formulation was centrifuged at 20,000 rpm for 15 minutes. Supernatant from formulation was kept in a separate tube, while the pellet (OTC-CS-CaCO₃NP) was washed, dried, and analyzed for morphological characteristics.

Morphological characterization of synthesized CS-CaCO₃NP and OTC-CS-CaCO₃NP

The average Zeta size, charge, and polydispersity index (PDI) of the synthesized CS-CaCO₃NP and OTC-CS-CaCO₃NP was done by dynamic light scattering technique using a Zetasizer Nano ZS, Malvern Instruments (Malvern Version 7.02, Malvern Instruments Ltd. UK). Briefly, 0.1 mg of freshly prepared CS-CaCO₃NP and OTC-CS-CaCO₃NP was dissolved in a test tube containing 10 ml of de-ionized water and was sonicated (Power Sonic 505®) for 20 minutes. 2 ml of the supernatant was gently aspirated into a syringe, fitted with a TRP® Spritzen-/syringe filter 0.45 µm and then fixed to the cuvette which was subsequently loaded into the machine. Measurements were taken in triplicates at a light scattering angle of 90° at 25°C.

The shape and particle size distribution of the synthesized CS-CaCO₃NP and OTC-CS-CaCO₃NP was determined using transmission electron microscopy (TEM) (IUPAC) while the surface morphology was done by field emission scanning electron microscopy (FESEM) equipped with an energy-dispersive X-ray spectroscopy unit. The specific surface area of CS-CaCO₃NP was determined by the Brunauer–Emmett–Teller (BET) technique via a 3-flex surface characterization analyzer (Micromeritics, Instrument Corporation, USA) using a total CS-CaCO₃NP weight of 0.2 g. X-ray powder diffractometer (Shimadzu XRD-6000 powder diffractometer) using CuKα (λ = 1.540562 Å) at 40 kV and 30 mA was used to investigate the crystallinity of CS-CaCO₃NP, OTC-CS-CaCO₃NP, and OTC alone. The crystallinity phase of the samples was done at different diffraction angles ranging from 2° to 60°, set at 0.02°/seconds in 2θ at 37°C (Saidykhani *et al.*, 2016). Functional group endings of the CS-CaCO₃NP, OTC-CS-CaCO₃NP, and OTC alone was determined using Fourier-transform infrared spectroscopy (Model 100 series, Perkin Elmer) at a range of 4,000 to 280 cm⁻¹ with a resolution of 2 cm⁻¹ and an average scan of 64 times.

Determination of OTC loading content and encapsulation efficiency

Six formulations of OTC-CS-CaCO₃NP loading were prepared. The first set comprised of three increasing doses of free OTC against the same three doses of CS-CaCO₃NP to make a 1:1, 2:1, and 3:1 ratio of OTC:CS-CaCO₃NP. The second set consists of three increasing doses of CS-CaCO₃NP with the same

three doses of free OTC in 1:2, 1:3, and 1:4 OTC:CS-CaCO₃NP ratio, respectively. The absorbance of the supernatants at 353 nm using ultraviolet-visible (UV-Vis) spectrophotometer (Shimadzu UV 1800) was measured and the concentration of the unloaded free OTC in all the supernatants was then determined using the equation generated from standard calibration curve for OTC at 353 nm (Fig. 1).

After which the loading content (LC) and encapsulation efficiency (EE) was calculated using Equations (1) and (2), respectively. The analyses of LC and EE was expressed as the mean percentage ± standard deviation (SD) based on two formulations that yielded similar results:

$$LC (\%) = \frac{W_t - W_f}{W_{np}} \times 100 \quad 1$$

$$EE (\%) = \frac{W_t - W_f}{W_t} \times 100 \quad 2$$

where W_t is the total weight of drug fed, W_f is the weight of non-encapsulated free drug, and W_{np} is the weight of nanoparticles. The results of drug loading were generated from the average of two independent experiments (Saidykhan *et al.*, 2016).

In vitro drug release study of the OTC form OTC-CS-CaCO₃NP

The profile of free OTC released from OTC-CS-CaCO₃NP was determined using the method of Chakraborty *et al.* (2012) with modifications. A total of 10 mg of free OTC and OTC-CS-CaCO₃NP was placed in a dialysis tube of 22 mm × 32 feet dry diameter (Thermo Scientific USA) and suspended in a glass jar containing 200 mL deionized water of four different pH (pH 4, 6, 7.4, and 8). The glass jar was covered and placed on a lab multistirrer (WiseCube® WIS-10; Wisd Laboratory Instruments, Witeg, Germany) at 37°C ± 0.5°C at 120 ± 1 rpm for 4 days (96 hours). At calculated time spans of 1 to 8 hours and then 24, 48, 72, and 96 hours, respectively, 1,000 µl of the solution was withdrawn and replaced by an equal amount of fresh deionized water of the equivalent pH to maintain a sink condition. The concentration of OTC released was determined at 353 nm (wavelength) using an UV-Vis spectrophotometer. The absorbance was interpreted according to an OTC standard calibration curve. The release study was conducted until there was an apparent total release of OTC. The percentage of OTC released was calculated based on the amount of OTC released at a given time to the amount of OTC loaded in OTC-CS-CaCO₃NP expressed mathematically below. The results obtained was plotted on a graph of cumulative percentage of drug release versus time intervals.

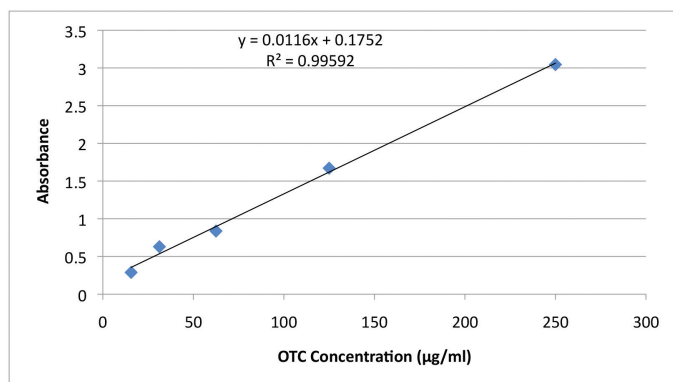


Figure 1. OTC standard curve at 353 nm.

$$\text{Amount of OTC released (mg)} = \frac{(\text{Concentration derived from standard curve mcg} \times \text{volume of dissolution medium})}{1000}$$

$$\text{Percentage OTC released} = \frac{\text{Amount of OTC released (mg)}}{\text{Total amount of OTC in OTC-CS-CaCO}_3\text{NP}} \times 100$$

$$\text{OTC-CS-CaCO}_3\text{NP} \times 100$$

$$\text{Cumulative percentage OTC released} = P(t-1) + P_t$$

where P_t = Percentage OTC released at time t ;
 $P(t-1)$ = percentage OTC released at time 1.

Statistical analysis

All data obtained were expressed as mean ± SD except for the elemental percentages which were expressed as mean ± standard mean of error (SEM).

RESULTS AND DISCUSSION

Zeta size, zeta potential, and polydispersity index (PDI)

The characterization of nanoparticles based on physicochemical properties such as size, shape, charge, and dispersity are important steps to understand its pharmacokinetics and biodistribution in biological medium (Murdock *et al.*, 2008). These physicochemical properties are the basic determinants of effective drug loading, controlled release, pharmacokinetics, efficacy, and toxicity, as well as bacterial cell internalization. Table 1 and Figures 2–5 show the zeta size, zeta potential, and PDI of CS-CaCO₃NP and OTC-CS-CaCO₃NP. The zeta size of CS-CaCO₃NP range from 93 to 98 nm while higher size (268–280 nm) was observed for OTC-CS-CaCO₃NP. The average zeta size (95.96 nm) of the synthesized CS-CaCO₃NP is within the limit (<100 nm) for which CaCO₃NP sizes <100 can be classified as nanometer-level particle, and this size usually enables the dispersion of drugs loaded within them (Pan *et al.*, 2018). Higher zeta size of 142 nm for CaCO₃NP has been reported

Table 1. Effect of dynamic light scattering on CS-CaCO₃NP and OTC-CS-CaCO₃NP.

Nanoparticle	Average Zeta size(nm)	Zeta potential	PDI
CS-CaCO ₃ NP	95.96 ± 2.7	-19.9 ± 1.27	0.36
OTC-CS-CaCO ₃ NP	276.00 ± 6.3	-23.5±1.10	0.33

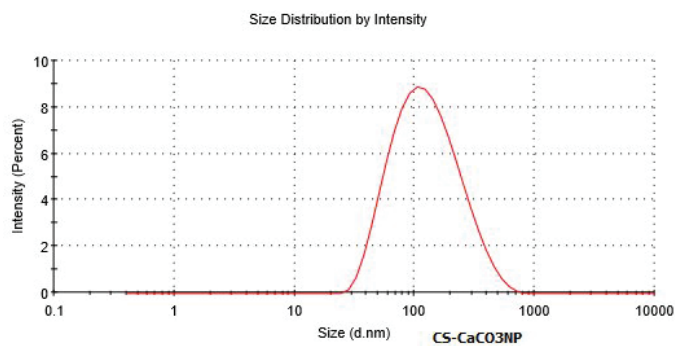


Figure 2. Zeta size distribution of CS-CaCO₃NP.

(Danmaigoro *et al.* 2017). The inclusion of BS-12 and longer period of milling ball impact on the power contributed to the lower zeta size and PDI observed. Higher size has always been associated with the agglomeration of the nanoparticles; however, the use of BS-12, a zwitterionic surfactant which acts as a capping agent, improved the dispersion of the CaCO_3NP , hence resulting in lower zeta size. The presence of a metal at a 90° angle in the ceramic jar increases the kinetic energy of the ceramic balls on one another as they strike the metal and further break the bonds in the CS- CaCO_3NP in the controlled energy ball milling mechanical process also contributed to further grind the CS- CaCO_3NP in the controlled energy ball milling mechanical process also contributed to further spreading and reducing the size of the nanoparticles generated from the cockle shell powder (Dhand *et al.*, 2015). Low PDI values have been reported for CS- CaCO_3NP from different studies (Isa *et al.*, 2016; Saikyhan *et al.*, 2016) and it is an indicator of the spread of size distribution of the nanoparticles (Faustino-Vega *et al.*, 2009; Masarudin *et al.*, 2015).

The zeta potential of CS- CaCO_3NP and OTC-CS- CaCO_3NP fall within the range (-25 mV and $+25$ mV) of aggregation for nanoparticles due to the weak Van Der Waal nanoparticle forces existing between the nanoparticles. The loading of oxytetracycline further increased the zeta charge almost close to the higher limit (Fig. 5) which requires greater force in bringing two particles together. A higher negative potential of OTC-CS- CaCO_3NP is suggestive of adsorption of negatively charged OTC on the internal surfaces of the CS- CaCO_3NP making the OTC-CS- CaCO_3NP more nano stable and remain longer in circulation with a reduced degree of agglomeration (Das *et al.*, 2011; Faustino-Vega *et al.*, 2009). The negative surface charge of CS- CaCO_3NP is also responsible for its interaction *in vivo* as negative nanoparticles have a prolonged systemic time compared to positive ones with very high clearance time (Arvizo *et al.*, 2011).

CS- CaCO_3NP and OTC-CS- CaCO_3NP morphology

The overall morphology of the synthesized nanoparticles was assessed using TEM and FESEM. The former providing information on particles size while the latter give shape and appearance (Liu *et al.*, 2010). The TEM revealed the average size of $29.90 \pm 6.3\text{nm}$ within the range of 17.6–41 nm for CS- CaCO_3NP (Figs. 6 and 7) while OTC-CS- CaCO_3NP showed a mean size of 62.4 ± 20.68 nm within the range of 23.02–81.50 nm (Figs. 8 and 9). Results of the FESEM analysis revealed a consistent spherical shape with a porous surface and solid or dense appearance for CS- CaCO_3NP and OTC-CS- CaCO_3NP , respectively (Figs. 10 and 11). The shape, size, and overall morphology of the CS- CaCO_3NP as seen on TEM and FESEM are important characteristics for effective loading of OTC into it by physical adsorption mechanism (Fu *et al.*, 2017). The solid-dense appearance of OTC-CS- CaCO_3NP indicates the presence of OTC within the nanoparticles. When comparing the zeta size with TEM size, it can deduce that both followed a similar pattern of low and high sizes for CS- CaCO_3NP and OTC-CS- CaCO_3NP , respectively. Although there is a marked difference in the actual sizes quoted by both techniques. The Zeta size measures the apparent size as the particles move in fluid (Brownian motion), thus measuring not only the particle but concentric layers of fluid around it (i.e., hydrodynamic diameter) resulting in exaggerated

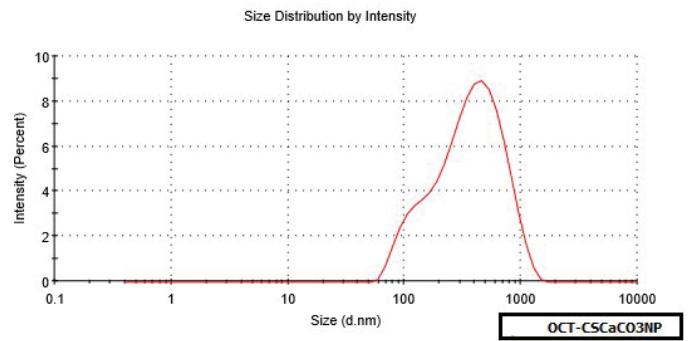


Figure 3. Zeta size distribution of OTC-CS- CaCO_3NP .

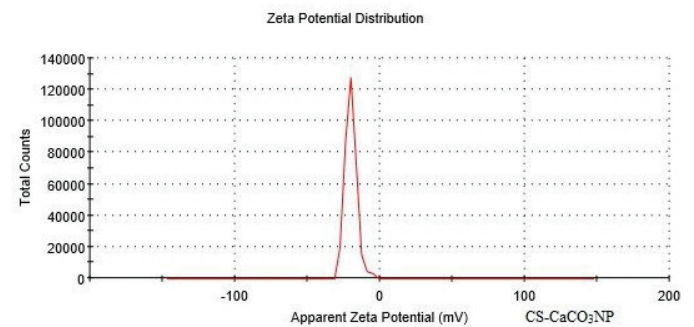


Figure 4. Zeta potential distribution of CS- CaCO_3NP .

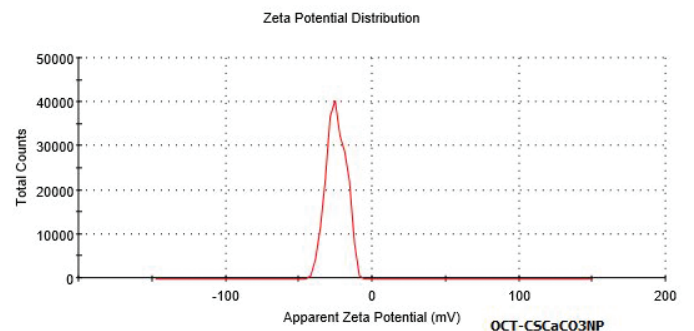


Figure 5. Zeta potential distribution of CS- CaCO_3NP .

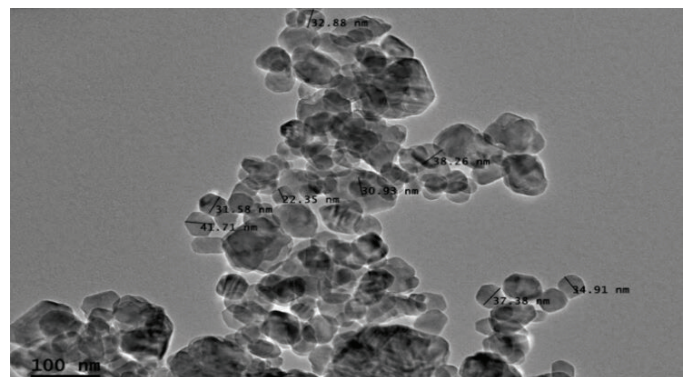


Figure 6. Photomicrograph of cockle shell derived calcium carbonate aragonite nanoparticle CS- CaCO_3NP on transmission electron microscope showing the nanoparticle sizes ranging from 17.6 to 41 nm.

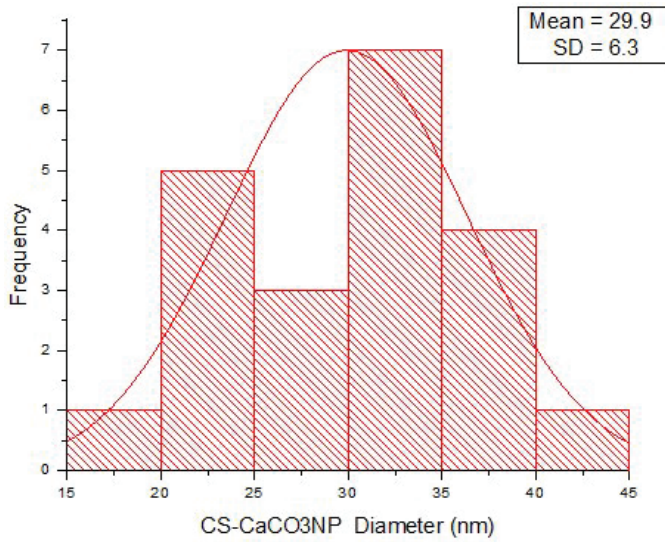


Figure 7. Average diameter, size, and distribution of CS-CaCO₃NP on TEM.

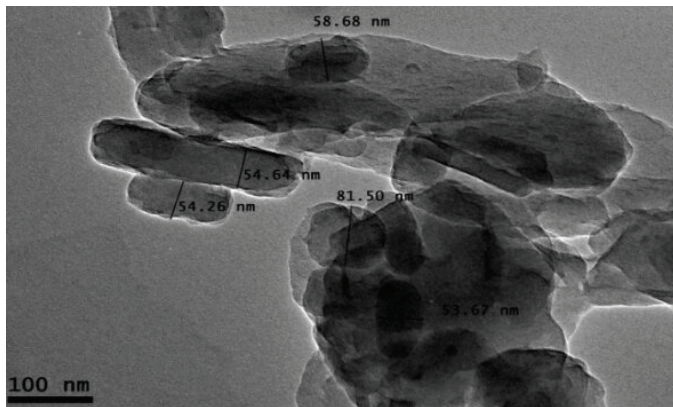


Figure 8. Photomicrograph of oxytetracycline loaded cockle shell derived calcium carbonate aragonite nanoparticle (OTC-CS-CaCO₃NP) on transmission electron microscope showing an average nanoparticle size of 53.73 nm.

size values. On the other hand, in TEM which is another method for measuring size, the air drying of CS-CaCO₃NP and OTC-CS-CaCO₃NP on the gold palladium after sonicating in distilled water during sample preparation resulted in a reduction in the size of the nanoparticles (Motwani *et al.*, 2008).

Elemental analysis of CS-CaCO₃NP and OTC-CS-CaCO₃NP (Tables 2 and 3) showed high amounts of oxygen, carbon, and calcium in decreasing order. This is in line with the chemical formula (CaCO₃) with oxygen being the highest. For CS-CaCO₃NP, carbon, oxygen, and calcium together account for 95.3% of the total elemental composition while the other elements (Mg, Na, Al, Si, and K) make up the remaining 4.7%. Similar findings were reported for C, O, and Ca by Kamba *et al.* (2013) and Islam *et al.* (2012). However, for OCT-CS-CaCO₃NP, the total elemental percentage for C, O, and Ca together is 91% while phosphorus alone is 5.6% and other elements (Na, Al, Si, K,

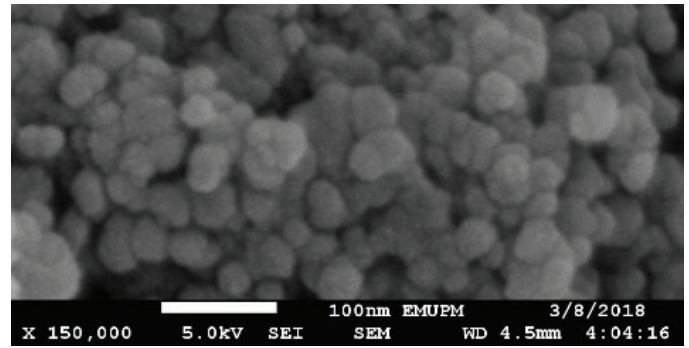


Figure 10. Field emission micrograph (FESEM) of spherically shaped CS-CaCO₃NP.

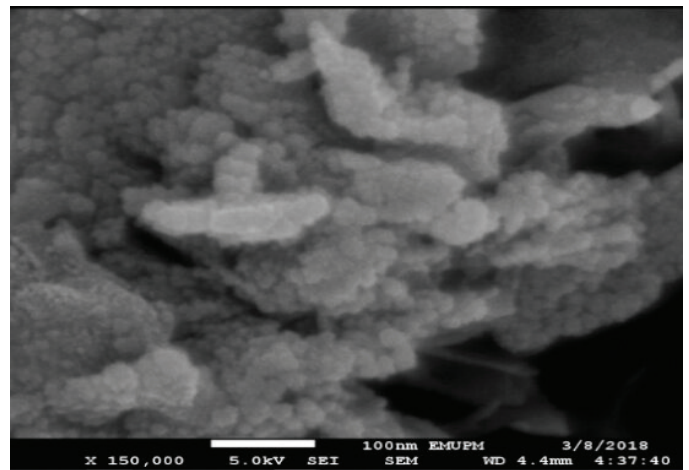


Figure 11. Field emission micrograph (FESEM) of spherically shaped OTC-CS-CaCO₃NP nanoparticle with the solid (dense) appearance.

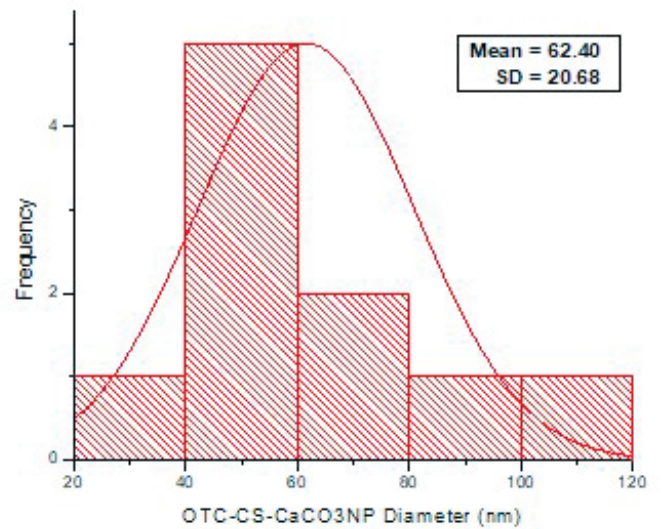


Figure 9. Average diameter, size, and distribution of OTC-CS-CaCO₃NP on TEM.

Table 2. Elemental analysis of CS-CaCO₃NP.

Spectrum	Ca	C	O	Na	Mg	Al	Si	K	Total
1	16.08	29.67	49.08	1.49	0.00	0.99	4.56	0.14	100
2	13.79	29.06	53.96	0.85	0.00	0.72	1.63	0.00	100
3	12.24	27.81	54.28	1.25	0.21	0.66	3.55	0.00	100
Mean	14.04	28.85	52.44	1.19	0.07	0.79	3.25	0.04	
±SEM	0.54	1.68	0.18	0.07	0.10	0.85	0.04	1.11	

Cl, and Cu) make the remaining 3.4%. The molecular formula of oxytetracycline hydrochloride is C₂₂H₂₅ClN₂O₉. Loading of OTC into CS-CaCO₃NP increased the percentage of carbon atoms while decreasing the amounts of oxygen and calcium present in CS-CaCO₃NP. The concentration of elements that makes up CaCO₃ is still high at 91% of the total amount of the elements that make up the nanoparticle loaded with drug loading with OTC did not change the composition of CS-CaCO₃NP.

FTIR and XRD analysis of CS-CaCO₃NP, OTC-CS-CaCO₃NP, and OTC

The characteristic vibration of the different functional groups present in CS-CaCO₃NP and OTC were explained by FTIR analysis (Fig. 12). CS-CaCO₃NP showed its most prominent peak at 1,452 cm⁻¹. This peak vibration corresponds to the alkyl group of CS-CaCO₃NP (Islam *et al.*, 2012; 2013) and is due to the C=O stretching vibration in the alkyl group. CO₃²⁻ peak that is characteristic of aragonite CS-CaCO₃NP were seen at 1,072.29, 854.77, and 707.58 cm⁻¹, respectively. The spectra of free OTC showed characteristic absorption bands at 1,010.64–1,622.76 cm⁻¹ which is attributed to the C=O and C=C bonds of the aromatic structure of OTC. The vibration at 1,622.76 cm⁻¹ is attributed to the C=N-H groups while that seen with peak at 3,317.91 is due to the N-H and N-C absorption bands of the amine group. The spectral bands of OTC-CS-CaCO₃NP which were attributed to the OTC are seen at 1,248.87–1,609 cm⁻¹, whereas bands located at 851, 938.43, 1,464, and 1,609.71 cm⁻¹ are those of amides while those at 1,020.03 and 1,248.87 are those resulting due to stretching of aromatic C=C. The bands seen between 1,200 and 1,600 cm⁻¹ in the free OTC are also present within the OTC-CS-CaCO₃NP bands. The characteristic CO₃²⁻ of aragonite CS-CaCO₃NP between 860.16 meaning that the OTC did not react significantly with the CS-CaCO₃NP following loading suggesting dispersion of OTC molecules within the OTC-CS-CaCO₃NP (Larbi-Bouamrane *et al.*, 2016).

The XRD diffractograms were done at 2θ peak position to identify fingerprints of the crystal phase of samples (Ni and Ratner, 2008). The XRD result pattern (Fig. 13) for CS-CaCO₃NP showed three strong peaks at 26.2°, 45.8°, and 33.1° at 2 θ degree

while that of OTC-CS-CaCO₃NP also showed three strong peaks at 31.8°, 32.4°, and 9.3°. These XRD diffractograms match with the International Centre for Diffraction Data database for aragonite crystals (JCPDS 00-141-1475). The appearance of two strong peaks of OTC-CS-CaCO₃NP very close to 33.1° is evidence that loading OTC into CS-CaCO₃NP did not affect the crystallinity of the CS-CaCO₃NP nanoparticle (Kamba *et al.*, 2013; Danmaigoro *et al.*, 2017). The first peak (9.5°) of free OTC corresponding to one of the strongest peaks in OTC-CS-CaCO₃NP is an indication that the drug is unaffected by loading into the nanoparticle.

BET surface area, average pore diameter, and total pore volume of CaCO₃NP

The curve derived from the linear isotherm plot of CaCO₃NP (Fig. 14) is convex to the P/Po axis throughout its range which qualifies it to be classified as the reversible Type III isotherm based on the IUPAC classification of adsorption isotherms (IUPAC, 1980). Classifying CaCO₃NP based on pore size, the average pore diameter (185 nm) is greater than 50 nm; hence, the pore size of the CaCO₃NP is biocompatible. The pore size is important for the adsorption of drugs into the nanoparticle because it enhances encapsulation efficiency and drug delivery (Xu *et al.*, 2018). The large surface area of 8.4987 ± 0.0922 (m²/g) of the CaCO₃NP compared to the pore volume 0.392931 (cm³/g) (Table 4) is an important unique characteristic of nanoparticles which allows for close interactions with other molecules compared to their bulked size counterparts. A large total pore volume of 0.392931 cm³/g is referred to as the adsorptive space (IUPAC, 1980).

Loading capacity and encapsulation efficiency of OTC

The LC and EE of the loaded OTC-CS-CaCO₃NP are shown in Table 5. Increasing concentrations of OTC resulted in increased loading capacity and encapsulation efficiency with maximal drug loss. Increasing concentrations of OTC resulted in increased LC and EE with maximal drug loss. This is because higher drug concentrations imply higher LC and EE but with increased loss of drugs outside the nanoparticle over the capacity than the nanoparticle can hold. While with increasing nanoparticle weight, there was decreasing LC with increased EE and minimal drug loss. This is because loading drugs into CS-CaCO₃NP is a function of the weight of drugs fed into the nanoparticles in relation to the weight of the nanoparticles (Abd Ghafar *et al.*, 2017; Muhamad and Selvakumaran, 2014). Incorporating drugs into CS-CaCO₃NP depends on capillary action and not on the surface charge and solubility of the drug (Jaji *et al.*, 2017). The negative charge of CS-CaCO₃NP may be responsible for the adsorption of OTC due to the electrostatic interaction with the positively charged quaternary ammonium functional group of the OTC

Table 3. Elemental analysis of OTC-CS-CaCO₃NP.

Spectrum	Ca	C	O	Ca	Al	Si	K	Cl	Cu	P	Total
1	7.90	36.23	46.25	1.95	0.85	0.55	0.10	0.82	0.16	5.18	100
2	8.18	36.87	45.09	2.04	0.95	0.52	0.00	0.87	0.00	5.49	100
3	9.36	39.96	40.33	1.93	0.93	0.40	0.00	0.96	0.00	6.14	100
Mean	8.48	37.69	43.89	1.97	0.91	0.49	0.33	0.88	0.05	5.60	100
±SEM	0.44	1.15	1.81	0.03	0.03	0.05	0.06	0.03	0.05	0.28	100

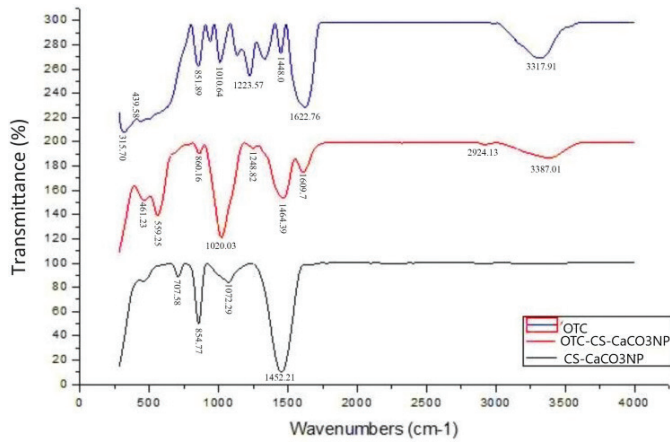


Figure 12. FTIR spectra of OTC, OTC-CS-CaCO₃NP, and CaCO₃NP.

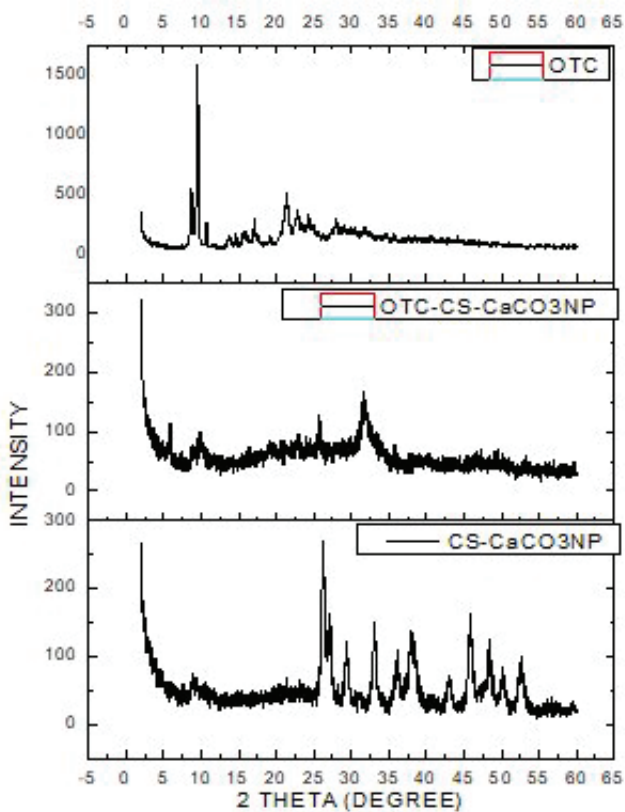


Figure 13. XRD spectra peak of OTC, OTC-CS-CaCO₃NP, and CaCO₃NP.

molecule (Harja and Ciobanu, 2018). Also, physical interaction like Van der Waals forces and hydrogen bonding between OTC and – COOH and – OH functional groups of CS-CaCO₃NP may have contributed to the adsorption of OTC into CS-CaCO₃NP (Deng *et al.*, 2013). The pores on the CS-CaCO₃NP leading to tortuous channels within the nanoparticles which the drug is carried into and loading of OTC into the CS-CaCO₃NP overnight could be responsible for the high loading capacity as the drug had been absorbed into the calcium carbonate nanoparticle resulting

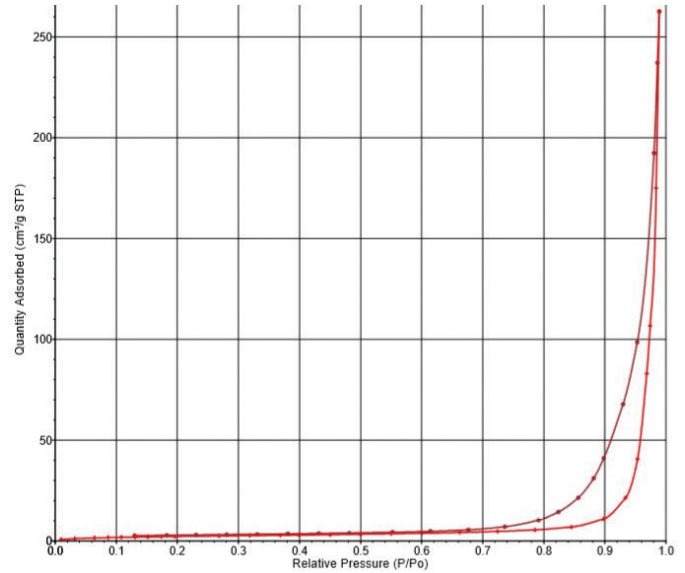


Figure 14. Adsorption-desorption isotherm linear plot of CaCO₃NP displaying the typical type III convex shape relative to the P/Po axis.

Table 4. BET surface area, average pore diameter, and total pore volume of CaCO₃NP.

Nanoparticle	BET surface area (m ² /g)	Average pore diameter (Å)	Total pore volume at P/Po = 0.988500000 (cm ³ /g)
CaCO ₃ NP	8.4987 ± 0.0922	1,849.3728	0.39

Table 5. Loading content and encapsulation efficiency of OTC-CaCO₃NP ratios.

OTC:CS-CaCO ₃ NP	Weight of OTC (mg)	Weight of CS-CaCO ₃ NP (mg)	Loading content (%)	Encapsulation efficiency (%)	PDI
1:1	5	5	71.2	71.2	0.32
2:1	10	5	171.4	85.7	0.33
3:1	15	5	268.8	89.6	0.35
1:2	5	10	35.8	71.6	0.31
1:3	5	15	23.9	71.7	0.33
1:4	5	20	17.9	71.8	0.31

expansion and subsequent increase in size and dark hollow centers seen in the OTC-CS-CaCO₃NP on TEM.

In vitro OTC release from OTC-CS-CaCO₃NP

The essence of loading drugs into carriers is not only to get them delivered to target sites but also ensure the maximum efficient release of the drug from the carrier so as to maintain a given concentration of the drug within the system during the course of therapy (Narayan *et al.*, 2012). Release study (Fig. 15) shows a fast release (99.4%) over 3 hours for free OTC at pH 4. The solubility of free OTC in deionized water makes it easier and faster to diffuse through the membrane to reach the medium from which the concentration was determined. However, for OTC-CS-CaCO₃NP, there was an initial rapid “burst” release from 0 to 8 hours, with a gradual and steady release over the rest of the 96 hours of the release profiles for the pH 4, 6, 7.4, and 8

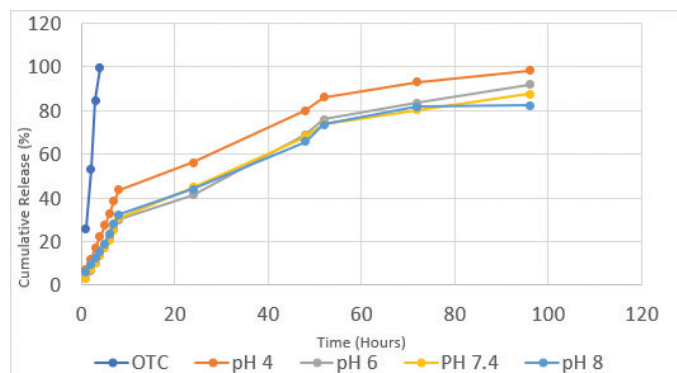


Figure 15. *In vitro* oxytetracycline release profile from OTC-CS-CaCO₃NP.

tested. The release was highest for pH 4 (98.2) and 6.0 (91.8%) when compared to pH 7.4 (87.7%) and 8.0 (82.4%). The release of OTC at different pH indicates that CS-CaCO₃NP is an efficient carrier which can maintain the concentrations of antibiotic during infections as compared to the free antibiotic release (Pan *et al.*, 2018). This high amount of OTC released from OTC-CS-CaCO₃NP at pH 4 may be attributable to the high solubility of OTC in acidic media as mentioned by Larbi-Bouamrane *et al.* (2016).

The slow release of OTC from OTC-CS-CaCO₃NP implies that encapsulation of OTC into colloids creates a better microenvironment which results in slow release of OTC over a longer period when compared with free OTC release (Faustino-Vega *et al.*, 2009). Furthermore, the initial burst release followed by the gradual steady release of OTC from OTC-CS-CaCO₃NP suggest that OTC-CS-CaCO₃NP is a core-shell structure (Xu *et al.*, 2011), with the OTC adsorbed on the surface (Shell) of CS-CaCO₃NP been released rapidly, while OTC loaded in the inner-core could only be released slowly from OTC-CS-CaCO₃NP via the pores through dissolution and diffusion (Larbi-Bouamrane *et al.*, 2016; Narayan *et al.*, 2012). Earlier studies of drug release from CS-CaCO₃NP showed slow decomposition and release rate at pH 7.4 and faster at pH > 6.5 (Dijaz *et al.*, 2015).

CONCLUSION

In the present study, OTC-CS-CaCO₃NP drug formulation was designed. The formulation was characterized morphologically and pharmacologically employing Zeta, FESEM, TEM, FTIR, XRD, and BET with drug loading and release studies. Mean size of CaCO₃NP and OTC-CS-CaCO₃NP was approximately 29.90 ± 6.30 and 62.40 ± 20.68, respectively, with sustained *in vitro* release at pH 4.0, 6.0, 7.4, and 8.0. Results from this work provide a basis to further probe the cytocompatibility and antibacterial effect of the synthesized OTC-CS-CaCO₃NP formulation.

FINANCIAL SUPPORT

This study was supported by Geran Putra, Universiti Putra Malaysia (Grant Code: GP/2018/9616700).

CONFLICTS OF INTEREST

The authors declare that there is no conflict of interest.

REFERENCES

- Abd Ghafar SLM, Hussein MZ, Zuki AZ. Synthesis and characterization of cockle shell-based calcium carbonate aragonite polymorph nanoparticles with surface functionalization. *J Nanoparticles*, 2017; 2017:1–12
- Adhikari MD, Goswami S, Panda BR, Chattopadhyay A, Ramesh A. Membrane-directed high bactericidal activity of (gold nanoparticle)–polythiophene composite for niche applications against pathogenic bacteria. *Adv Healthc Mater*, 2013; 2:599–606.
- Arviso RR, Miranda OR, Moyano DF, Walden CA, Giri K, Bhattacharya R, Robertson JD, Rotello VM, Reid JM, Mukherjee P. Modulating pharmacokinetics, tumor uptake and biodistribution by engineered nanoparticles. *PLoS One*, 2011; 6:3–8.
- Chakraborty SP, Sahu SK, Pramanik P. Biocompatibility of folate-modified chitosan nanoparticles. *Asian Pac J Trop Biomed*, 2012; 2:215–9.
- Danmaigoro A, Selvarajah GT, Hezmee MNM, Mahmud R, Zuki AZ. Development of cockleshell (*Anadara granosa*) derived CaCO₃ nanoparticle for doxorubicin delivery. *J Comput Theor Nanosci*, 2017; 14:5074–86.
- Das S, Chaudhury A. Recent advances in lipid nanoparticle formulations with solid matrix for oral drug delivery. *AAPS Pharm Sci Tech*, 2011; 12:62–76.
- Deng, H, Shen XC, Wang XM, Du C. Calcium carbonate crystallization controlled by functional groups: a mini-review. *Front Mater Sci*, 2013; 7(1); doi 10.1007/s11706-013-0191-y
- Dhand C, Dwivedi N, Loh XJ, Ying ANJ, Verma NK, Beuerman RW, Lakshminarayanan R, Ramakrishna S. Methods and strategies for the synthesis of diverse nanoparticles and their applications: a comprehensive overview. *RSC adv*, 2015; 5:105003–37.
- Dijaz SM, Jalali MB, Zarrintan MH, Adibkhia KM, Lotfipour F. Calcium carbonate nanoparticles as cancer drug delivery system. *Expert Opin Drug Deliv*, 2015; 12:1649–60.
- Faustino-Vega A, Alvarez-Polo MA, Gasca B, Bernad-Bernad M. Influence of three different colloidal systems on the oxytetracycline-lecithin behaviour. *Pharmazie*, 2009; 64:505–9.
- Fu W, Hezmee MNM, Yusof LM, Ibrahim TAT, Keong YS, Jaji AZ, Zuki AZ. *In vitro* evaluation of a novel pH sensitive drug delivery system-based cockle shell-derived aragonite nanoparticles against osteosarcoma. *J Exp Nanosci*, 2017; 12:166–87.
- Harja M, Ciobanu G. Science of the total environment studies on adsorption of oxytetracycline from aqueous solutions onto hydroxyapatite. *Sci Total Environ*, 2018; 628–629:36–43.
- Isa T, Zuki AZ, Rukayadi Y, Hezmee MNM, Jaji AZ, Imam MU, Hammadi IN, Mahmood SK. Antibacterial activity of ciprofloxacin-encapsulated cockle shells calcium carbonate (aragonite) nanoparticles and its biocompatibility in macrophage J774A. *IJMS*, 2016; 17:713–30.
- Islam KN, Zuki AZ, Ali ME, Hussein MZB, Noordin MM, Loqman MY, Islam A, Islam MS, Rahman MM, Ullah M. A novel method for the synthesis of calcium carbonate (aragonite) nanoparticles from cockle shells. *Powder Technol*, 2013; 235:70–5.
- Islam KN, Zuki AZ, Ali ME, Hussein MZB, Noordin MM, Loqman MY, Wahid H, Hakim MA, Abd Hamid SB. Facile synthesis of calcium carbonate nanoparticles from cockle shells. *J Nanomater*, 2012; 2012:1–5.
- IUPAC. Commission on colloid and surface chemistry including catalysis. *Pure Appl Chem*, 1982; 11:2201–18.
- Jaji AZ, Zuki AZ, Mahmud R, Loqman MY, Hezmee MNM, Isa T, Wenliang F, Hammadi IN. Synthesis, characterization, and cytocompatibility of potential cockle shell aragonite nanocrystals for osteoporosis therapy and hormonal delivery. *Nanotechnol Sci Appl*, 2017; 1:23–33.
- Kamba S, Ismail M, Hussein-Al-Ali S, Ibrahim T, Zuki AZ. *In Vitro* delivery and controlled release of doxorubicin for targeting osteosarcoma bone cancer. *Molecules*, 2013; 18:10580–98.

Larbi-Bouamrane O, Bal Y, Aliouche D, Cote G, Chagnes A. Preparation and Characterization of cross-linked chitosan microcapsules for controlled delivery of oxytetracycline. *Indian J Pharm Sci*, 2016; 78:715–24.

Liu F, Wu J, Chen K, Xue D. Morphology study by using scanning electron microscopy. In: Méndez-Vilas A, Díaz, J (eds.). *Science, technology, applications and education*, Formatex Research Center, Badajoz, Spain, vol 3, pp 1783–92.

Masarudin MJ, Cutts SM, Evison BJ, Pigram PJ. Factors determining the stability, size distribution, and cellular accumulation of small monodisperse chitosan nanoparticles as candidate vectors for anticancer drug delivery: application to the passive encapsulation of [14 C]-doxorubicin. *Nanotechnol Sci Appl*, 2015; 8:67–80.

Motwani SK, Chopra S, Talegaonkar S, Kohli K, Ahmad FJ. Chitosan-sodium alginate nanoparticles as submicroscopic reservoirs for ocular delivery: formulation, optimisation and *in vitro* characterisation. *Eur J Pharm Biopharm*, 2008; 68:513–25.

Muhamad II, Selvakumaran S. Designing polymeric nanoparticles for targeted drug delivery system outline. *Nanomedicine*, 2014; 11:287–313.

Murdock RC, Braydich-Stolle L, Schrand AM, Schlager JJ, Hussain SM. Characterization of nanomaterial dispersion in solution prior to *in vitro* exposure using dynamic light scattering technique. *Toxicol Sci*, 2008; 101:239–53.

Narayanan D, Anitha A, Jayakumar R, Nair SV, Chennazhi KP. Synthesis, characterization and preliminary *in vitro* evaluation of PTH 1-34 loaded chitosan nanoparticles for osteoporosis. *J Biomed Nanotech*, 2012; 8:98–106.

Ni M, Ratner B. Differentiation of calcium carbonate polymorphs by surface analysis technique – An XPS and TOF-SIMS study. *Surf Interface Anal*, 2008; 40:1356–61.

Othman NH, Abu Bakar BH, Don MM, Johari MAM. Cockle shell ash replacement for cement and filler in concrete. *MJCE*, 2013; 25:200–11.

Pan X, Chen S, Li D, Rao W, Zheng Y, Yang Z. The Synergistic antibacterial mechanism of gentamicin-loaded CaCO₃ nanoparticles. *Front Chem*, 2018; 5:1–9.

Priyadarshana G, Kottegoda N, Senaratne A, deAlwis A, Karunaratne V. Synthesis of magnetite nanoparticles by top-down approach from a high purity ore. *J Nanomater*, 2015; 1–8.

Rawat P, Rajput YS, Bharti MK, Sharma RA. Method for synthesis of gold nanoparticles using 1-amino-2-naphthol-4-sulphonic acid as reducing agent. *Curr Sci*, 2016; 110:2297–300.

Razalia NIM, Pramanika S, Abu Osmana N, Radzib Z, Pingguan-Murphy B. Conversion of calcite from cockle shells to bioactive nanorod hydroxyapatite for biomedical applications. *J CPR*, 2016; 17:699–706.

Saidykhan L, Zuki AZ, Rukayadi Y, Kura AU, Latifah SY. Development of nanoantibiotic delivery system using cockle shell-derived aragonite nanoparticles for treatment of osteomyelitis. *IJN*, 2016; 11:661–73.

Xu W, Pengjin G, Zhang N, Liu X, Xie J. Macroporous silica nanoparticles for delivering Bcl2-function converting peptide to treat multidrug resistant-cancer cells. *J Colloid Interface Sci*, 2018; 527:141–50.

Xu X, Wang Y, Chen R, Feng C, Yao F, Tong S, Wang L, Yamashita F, Yu J. Formulation and pharmacokinetic evaluation of tetracycline-loaded solid lipid nanoparticles for subcutaneous injection in mice. *Chem Pharm Bull*, 2011; 59:260–5.

How to cite this article:

Idris SB, Arifah AK, Jesse FFA, Ramanoon SZ, Basit MA, Zakaria ZA, Zakaria MZAB. Synthesis, characterization, and *in vitro* release of oxytetracycline loaded in pH-responsive CaCO₃ nanoparticles. *J Appl Pharm Sci*, 2019; 9(11):019–027.